JACS
JOURNAL OF THE AMERICAN CHEMICAL SOCIETY
Article
pubs.acs.org/JACS

Chemical Mustard Containment Using Simple Palladium Pincer Complexes: The Influence of Molecular Walls

Qi-Qiang Wang, Rowshan Ara Begum, Victor W. Day, and Kristin Bowman-James*

Department of Chemistry, University of Kansas, Lawrence, Kansas 66045, United States

Supporting Information

ABSTRACT: Six amide-based NNN palladium(II) pincer complexes Pd(**L**)(CH_3CN) were synthesized, characterized, and examined for binding the sulfur mustard surrogate, 2-chloroethyl ethyl sulfide (CEES). The complexes all bind readily with CEES as shown by ^{1}H NMR spectroscopy in $CDCl_3$. The influence of para-substituents on the two amide phenyl appendages was explored as well as the effect of replacing the phenyl groups with larger aromatic rings, 1-naphthalene and 9-anthracene. While variations of the para-substituents had only a slight influence on the binding affinities, incorporation of larger aromatic rings resulted in a significant size-related increase in binding, possibly due to increasing steric and electronic interactions. In crystal structures of three CEES-bound complexes, the mustard binds through the sulfur atom and lies along the aromatic walls of the side appendages approximately perpendicular to the pincer plane, with increasingly better alignment progressing from phenyl to 1-naphthalene to 9-anthracene.

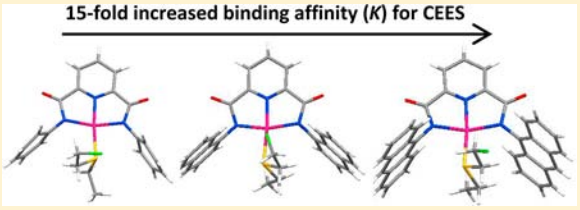

INTRODUCTION

Interest in the chemical mustards began as a result of their toxic properties and use as chemical warfare agents in World War I.[1] Hence, in the early half of the 20th century considerable research was directed toward unraveling the complex chemistry of these harmful agents.[2] Yet findings that they also have value in therapeutical applications, particularly the amine-based mustards, such as in chemotherapy first in the 1940s[3] and more recently as well,[4] have revived interest in their chemistry.

The original mustard gas, 2,2′-dichlorodiethyl sulfide, has a number of variants, including the nitrogen mustards, 2,2′-dichlorodiethylamines, and the half sulfur mustard, 2-chloroethyl ethyl sulfide (CEES).[2] Much of the chemistry of the mustards involves the electrophilic nature of the β-CH_2 groups, which undergo either intramolecular or intermolecular nucleophilic attack.[2,5] Consequently, these reactive molecules can alkylate important cellular components such as DNA, RNA, and proteins, which leads to their cytotoxicity.[6]

While considerable research has been devoted to exploring ways to decontaminate the mustards,[7] current efforts also focus on their medicinal potential.[8] Hence, timely challenges include both a better understanding of mustard chemistry and the development of efficient artificial receptors for their detection and decontamination as well as for binding and delivery.[9−11]

In the course of developing receptor systems for the half sulfur mustard, CEES, with palladium(II) pincer complexes, we uncovered significantly enhanced binding when naphthalene and anthracene walls were used to align with the bound linear guest. In short, extended aromatic side appendages provide effective containment for the pseudolinear CEES guest (Scheme 1).

Scheme 1. Amide Substituents in the NNN Pincer Skeleton

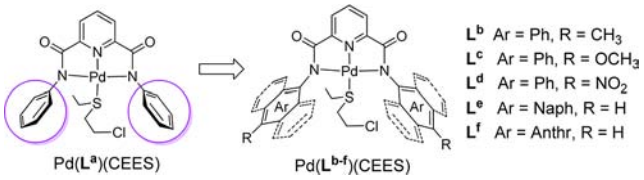

Pincer ligands are relatively rigid tridentate chelates typically composed of a central donor atom from a phenyl ring or other heterocycle (e.g., pyridine) plus two side ortho-substituted donor atoms.[12] Pincer complexes with a variety of transition metal ions have been of broad interest because of their versatile chemistry, including applications in catalysis, sensing, and materials research.[12−14] The key to the reactivity of these complexes lies in the general lability of the fourth coordination site. Upon initial isolation, the fourth site is usually occupied by a counterion or solvent molecule, which can be replaced by a stronger ligand.[15−18]

Recently we reported SNS thioamide-based platinum(II) pincer complexes as proton switches for the half sulfur mustard (CEES), along with preliminary studies of the amide-based system reported here.[19] The SNS platinum(II) complexes undergo reversible thioamide ↔ iminothiolate transformations with base followed by acid, which accordingly leads to the reversible binding ↔ release of CEES at the fourth coordination site.

Preliminary studies, including a crystal structure, on a corollary amide-based NNN palladium(II) pincer revealed

Received: August 23, 2013
Published: October 4, 2013

   dx.doi.org/10.1021/ja408770u | J. Am. Chem. Soc. 2013, 135, 17193−17199

that it also binds CEES, but without the switch-like mechanism. Because of the relative synthetic ease of synthesizing modified appendages in this class of ligand systems, we decided to explore the electronic and steric influences of the ligand periphery on CEES binding. Herein we report the structural and binding results, along with the unanticipated binding enhancements afforded by peripheral "walls".

RESULTS AND DISCUSSION

Synthesis. The *N*,*N*′-disubstituted pincer ligands, H_2**L**, were synthesized by reacting 2,6-pyridinedicarbonyl dichloride with 2 equiv of the corresponding amines in high yields (70−92%) using commonly accepted procedures.[14,19] The synthesis of the NNN palladium(II) pincer complexes Pd(**L**)(CH_3CN) is straightforward by reacting H_2**L** with 1 equiv of $Pd(AcO)_2$ in acetonitrile at room temperature for several days as reported previously (see Supporting Information).[16,19] After the reaction, the products were directly obtained by filtration and recrystallized from acetonitrile if necessary to give pure compounds in 51−99% yields.

The CEES complexes used for the studies were obtained in two different ways. For the binding studies, the precursor complexes were dissolved in $CDCl_3$ followed by titration with various equivalents of CEES. For crystals suitable for X-ray analysis, the acetonitrile complexes were dissolved in neat CEES, and crystallized over a period of time (ranging from a few hours to a couple of days). All of the precursor complexes Pd(**L**)(CH_3CN) were fully characterized by mass spectrometry (MS), ^{1}H NMR spectroscopy, and elemental analysis. The DMF complex of the free ligand H_2**L**^{f}, three of the acetonitrile precursors, and three of the CEES adducts were crystallographically characterized. The transformation equilibrium in solution upon addition of the CEES to the acetonitrile precursors was investigated by ^{1}H NMR in $CDCl_3$ (vide infra).

NMR Studies. *Solution NMR.* The ^{1}H NMR of the simplest phenyl-appended Pd(**L**^{a})(CH_3CN) was poorly resolved and is probably attributed to the coexistence of an equilibrium between the monomeric complex and a cyclic hexamer $[Pd(\mathbf{L}^a)]_6$ in solution (Scheme 2 and Figure S1, Supporting Information). Crystallographic results for crystals isolated from the reaction mixture after sitting overnight confirmed the formation of a hexamer, the structure and chemistry of which was reported by us recently.[20] Although the presence of the hexamer tends to affect the resolution of the spectrum, the signals for free and bound acetonitrile are clear and appear at 2.01 and 1.74 ppm, respectively, for the phenyl derivative (Table 1 and Figure S1, Supporting Information). The upfield shifts are probably due to the shielding effect by adjacent phenyl rings. In fact, while this signal in the phenyl and substituted phenyl derivatives, **L**$^{a-c}$ (**L**^{d} being sparingly soluble), ranges from 1.74 to 1.80 ppm, in the extended aromatic naphthalene and anthracene derivatives, **L**^{e} and **L**^{f}, the signals are shifted even higher upfield by approximately 1.2 and 1.7 ppm, respectively. Such an observation tends to support the enhanced shielding in the extended π systems. For Pd(**L**^{e,f})-(CH_3CN), clear and resolved spectra were immediately observed upon dissolution of the sample, indicating that the cyclization process does not occur, most probably due to the steric bulk of the expanded aromatic systems (see Supporting Information).

Upon stepwise addition of CEES to fresh solutions of the complexes Pd(**L**)(CH_3CN) in $CDCl_3$, the proton signals of the bound acetonitrile gradually disappeared. The signal for free acetonitrile continued to grow upon subsequent addition of CEES, as well as a new set of signals corresponding to coordinated CEES (see Supporting Information). After addition of 2 equiv of CEES, the acetonitrile complexes were almost entirely converted to the CEES complexes (Figure 1). As with the acetonitrile complexes, upon binding, the CEES signals shifted upfield due to shielding by the aromatic rings. For Pd(**L**$^{a-c}$)(CEES) these shifts were most pronounced for the two methylene groups coordinated with the central sulfur atom, CH_2^b and CH_2^c (approximately 0.8 ppm compared to about 0.1−0.25 ppm for CH_2^a and CH_2^d), and the magnitude of the chemical shift changes decreased slightly along the series R = H > CH_3 > OCH_3 (Table 1). The chemical shift changes for the naphthalene- and anthracene-based complexes, **L**^{e} and **L**^{f}, increased dramatically, most strikingly for the anthracene derivative. For the latter complex, the changes are almost double those seen in the naphthalene complex, indicating the powerful effect of the extended π system. The NMR spectrum of the naphthalene derivative is complicated by the presence of isomers as described in greater detail below.

Naphthalene Isomers. Compared with the other precursors, the NMR spectrum of the naphthalene complexes was complicated by the coexistence of the two stereoisomers, cis and trans, corresponding with the two side naphthalene rings oriented in the same (cis) or opposite (trans) direction (Scheme 3). The possible enantiomers due to the potential planar chirality are not shown. The presence of the isomers is evident by the observation of two signals for the bound acetonitrile methyl group at 0.84 and 0.80 ppm (Figure 2). Also, two independent doublet signals at 8.46 and 8.39 ppm (denoted by * and *′) exist for one of the naphthalene aromatic protons, each integrating to one proton. Other naphthalene signals are also split but are too complex to unravel. The nearly equal integration of the corresponding signals suggests an approximate 1:1 cis:trans composition.

Upon binding CEES, the NMR spectrum of the dissymmetric molecule becomes more complex. Theoretically, signals due to the three stereoisomers (**A**, **B**, and **C**) should exist with three distinct NMR spectra (Scheme 3). However, signals for

Scheme 2. ChemDraw Depiction of the Binding of CEES with Pd(L^a)(CH_3CN) Showing H-Atom Assignments for CEES

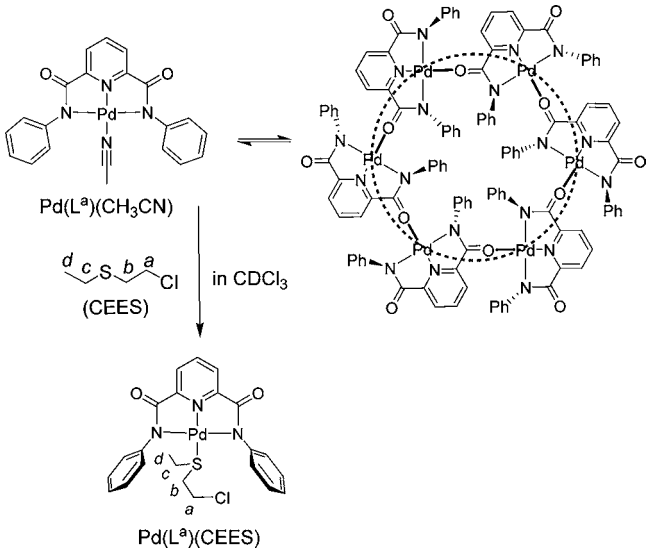

dx.doi.org/10.1021/ja408770u | J. Am. Chem. Soc. 2013, 135, 17193−17199

Table 1. ^{1}H NMR Chemical Shifts (δ, ppm)[a] of the Bound CH_3CN and CEES in the Complexes Pd(L)(X) (X = CH_3CN and CEES)

	X = CH_3CN	X = CEES			
	CH_3CN	$ClCH_2$[a]	$ClCH_2CH_2$[b]	$CH_2^cCH_3$	CH_2CH_3[d]
unbound	2.01	3.64	2.87	2.60	1.28
L^a	1.74(0.27)	3.40(0.24)	2.03(0.84)	1.83(0.77)	1.13(0.15)
L^b	1.77(0.24)	3.44(0.20)	2.06(0.81)	1.87(0.73)	1.15(0.13)
L^c	1.80(0.21)	3.46(0.18)	2.10(0.77)	1.90(0.70)	1.17(0.11)
L^e[b]	0.84(1.17) 0.80(1.21)	2.83(0.81) 2.86(0.78)	1.43(1.44) 1.44(1.43)	1.10(1.50) 1.11(1.49)	0.63(0.65) 0.66(0.62)
L^f	0.33(1.68)	2.20(1.44)	0.75(2.12)	0.32(2.28)	0.07(1.21)

[a]The $\Delta\delta$ values ($\delta_{unbound} - \delta_{bound}$) are shown in the brackets. [b]Two sets of stereoisomer signals were observed for Pd(L^e)(CH_3CN) and Pd(L^e)(CEES). In the latter, the signals were complicated in the 400 MHz NMR spectrum but can be clearly elucidated by 800 MHz NMR (see Figure 3): left, cis-isomer **A**/**B**; right, trans-isomer **C**, where the average value of the two nonequal protons CH^1 and CH^2 on each carbon atom is shown.

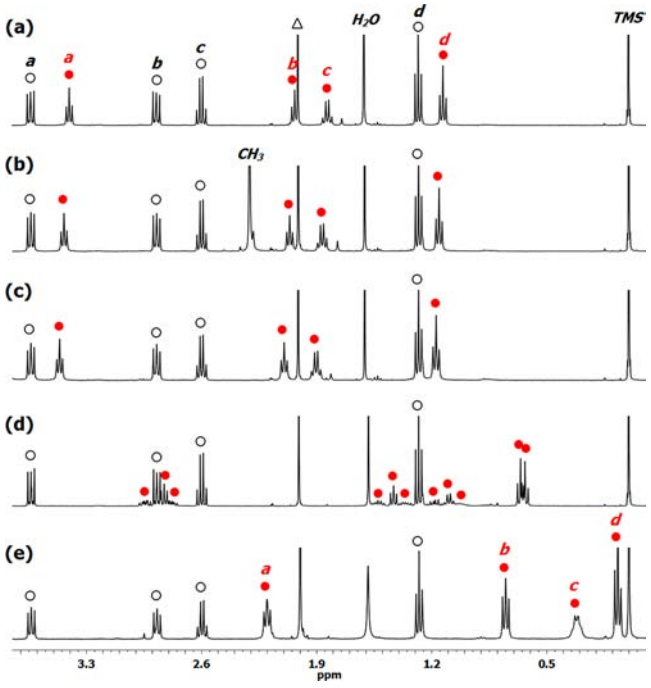

Figure 1. Partial ^{1}H NMR (400 MHz, 298 K, $CDCl_3$) of Pd($L^{a,b,c,e,f}$)(CH_3CN) (10 mM) after adding 2 equiv of CEES: (a) L^a, (b) L^b, (c) L^c, (d) L^e and (e) L^f. Resonance designations Δ, ○, and red solid circle correspond to the signals of free CH_3CN, and free and bound CEES, respectively. See Scheme 2 for representative H-atom assignments.

Scheme 3. Possible Stereoisomers for Pd(L^e)(CH_3CN) and Pd(L^e)(CEES)

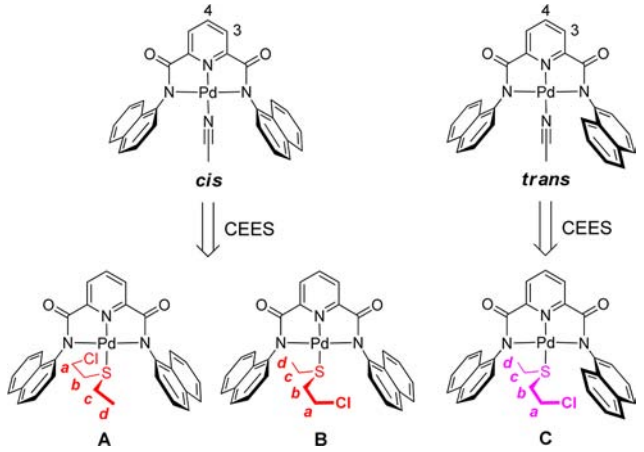

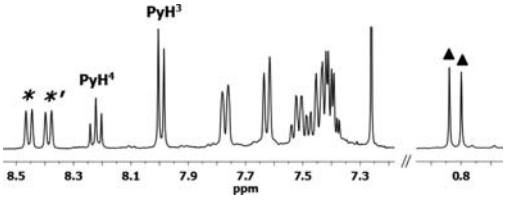

Figure 2. Partial ^{1}H NMR (400 MHz, 298 K, $CDCl_3$) of Pd(L^e)(CH_3CN). Resonance designation ▲ corresponds to the bound CH_3CN signals. See Scheme 3 for the structures of the cis and trans stereoisomers.

only two isomers, cis and trans, were identified, although a three-signal pattern is observed for CEES protons CH_2^{a-c}. Within each of these sets, one of the three signals exhibits approximately twice the integration as each of the other two (Figure 1d). As seen in the higher resolution of the 800 MHz NMR spectrum (Figure 3), the signals become more resolved and are assigned to the undifferentiated cis **A**/**B** isomer (in red) and the trans **C** isomer (in magenta). The more intense set of three triplets and a quartet is assigned to the cis isomer. While it could be ascribed to **A** and/or **B**, the 2D NOESY experiment shows cross peaks between the hydrogen atoms at both the 2- and 8-positions of the naphthalene with all four of the hydrogen atom signals on the mustard (Figure S7, Supporting Information). These solution structural effects, including isomerization reactions, are being investigated further.

The second set of less intense signals consists of six complex multiplets (some of which can be recognized as octets) and one more intense clearly defined triplet at about 0.66 ppm. The latter signal is assigned to the terminal methyl group. The breakdown of individual hydrogen atoms attached to the same carbon for the other signals is a result of the diastereotopic $Cl(CH^1H^2)_a(CH^1H^2)_bS(CH^1H^2)_c(CH_3)_d$ system (see inset in Figure 3), which was further confirmed by a 2D ^{1}H−^{1}H COSY experiment (Figure S6, Supporting Information). This assignment is consistent with the trans-isomer **C** which is C_1 or no symmetry. For this isomer, the two protons on each CH^1H^2 group would be nonequivalent due to the different magnetic shielding environments provided by the trans, staggered naphthalene rings.

About 5 min after the addition of CEES to a solution of Pd(L^e)(CH_3CN) in $CDCl_3$, the concentration of cis-isomers is slightly in excess compared to trans (**A**/**B**:**C** = 52:48). However, upon initial mixing (when the complex may not

dx.doi.org/10.1021/ja408770u | J. Am. Chem. Soc. 2013, 135, 17193−17199

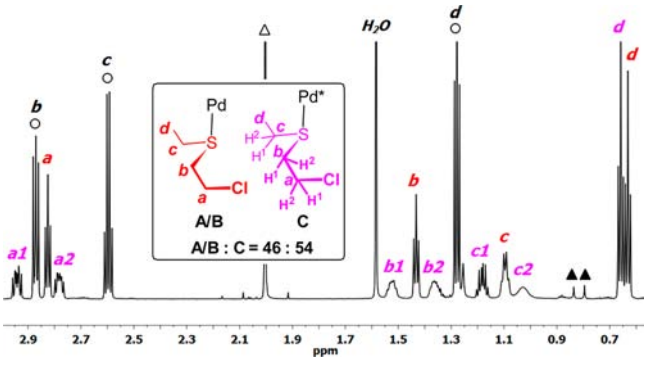

Figure 3. Partial 800 MHz ^{1}H NMR (298 K, $CDCl_3$) of Pd(**L**^{e})(CH_3CN) (10 mM) with addition of ca. 2 equiv of CEES after reaching an equilibrium. Resonance designations Δ , ▲, and ○ correspond to the signals of free and bound CH_3CN, and free CEES, respectively. See Scheme 3 for the complete structures of the stereoisomers **A**, **B**, and **C**.

yet be completely dissolved), the ratio of cis:trans isomers is considerably higher. A slow conversion to a slight excess of trans-isomer is reached within ca. 2 h (Figure S8, Supporting Information). The predominance of the cis isomers early in the reaction may be due to the less restricted approach of the mustard at the axial site away from the naphthalenes in the anticipated associative mechanism for square planar substitution reactions. Upon reorganization after CEES binding, one or both of the naphthalene groups apparently rotates, resulting in the different isomer ratios.

Binding Studies. ^{1}H NMR studies were used to investigate electronic and steric effects of different amide substituents on CEES binding. All the complexes were tested except Pd(**L**^{d})(CH_3CN), which was not very soluble. Equilibrium constants K (eq 1) for the remaining five Pd(**L**)(CH_3CN) complexes were measured in $CDCl_3$ (Table 2). While the naphthalene complex, Pd(**L**^{e}), consists of cis and trans isomers, we were interested in the equilibrium constant for the entire complex, not the individual isomers. Thus, the hydrogen on the pyridine carbon atom, C^3 (Scheme 3), which was not split due to the isomers, was used for determining the K.

Table 2. Binding Affinities (K)^a of CEES with the Pincer Complexes Pd(L)(CH_3CN)

	L^a	**L**^{b}	**L**^{c}	**L**^{e}	**L**^{f}
K	15	20	25	76	220
log K	1.16	1.31	1.39	1.88	2.34

^{a}Determined by ^{1}H NMR in $CDCl_3$. In each case, three parallel measurements were taken and an average K value is given; error <10%.

$$\mathrm{Pd(L)(CH_3CN)} + \mathrm{CEES} \overset{K}{\rightleftharpoons} \mathrm{Pd(L)(CEES)} + \mathrm{CH_3CN}$$

$$K = \frac{[\mathrm{Pd(L)(CEES)}][\mathrm{CH_3CN}]}{[\mathrm{Pd(L)(CH_3CN)}][\mathrm{CEES}]} \quad (1)$$

CEES binds rapidly, reaching equilibrium almost immediately upon mixing Pd(**L**)(CH_3CN) and CEES in $CDCl_3$. The equilibrium can be shifted slightly back by deliberately adding a few microliters of acetonitrile to the solution. For determination of the binding constant, K, the relative concentration ratios of the four equilibrium species in the solution were obtained by integrating the representative ^{1}H signals. The presence of any hexameric species (in the case of **L**$^{a-c}$) was deemed negligible in the equilibrium solutions used for the determination of K due to the presence of a strongly coordinating ligand (CEES).

All five pincer complexes were found to bind (K > 10) CEES; however, the magnitude varied significantly across the series. The *p*-CH_3 (**L**^{b}) and *p*-OCH_3 (**L**^{c}) substituents resulted in only slightly increased CEES binding constants, which could be the result of either electronic effects or possibly structural influences of the added para substituents. However, incorporation of larger aromatic rings at the pincer periphery significantly enhanced CEES binding (Table 2). The crystal structures of the series of three complexes (**L**^{a}, **L**^{e}, and **L**^{f}) shed light on this interesting increase, which may be both electronic and structural in nature. The structures may also help to explain the rather large upfield chemical shifts seen for the bound CEES in both the naphthalene- and anthracene-containing complexes as described in greater detail below.

Crystallographic Studies. *Pd(L)(CEES) Complexes.* The crystal structure results of Pd(**L**^{a})(CEES) were communicated previously,[19] but the salient features are described here for comparative purposes with the two new crystal structures. Crystal structures were also obtained for three of the acetonitrile precursor complexes as well as the DMF solvate of the free base of H_2**L**^{f} (see Supporting Information).

Common trends for pincers are observed for all three of the CEES complexes, including the rather short Pd–N(1) distance ranging from 1.94 to about 1.96 Å and longer bonds (by almost exactly 0.1 Å in each case) to the amide nitrogen atoms (Table 3). The Pd–N1 distances are longer for the mustard structures

Table 3. Coordinated Bond Distances (Å) and Dihedral Angles (deg) for the NNN–Pd–CEES Pincer Complexes

		Pd(**L**^{e})(CEES)		
	Pd(**L**^{a}) (CEES)	**A/B**	**C**	Pd(**L**^{f}) (CEES)
Pd–N1	1.940(11)	1.957(5)	1.953(5)	1.954(3)
Pd–N2	2.040(9)	2.051(6)	2.049(6)	2.054(3)
Pd–N3	2.029(9)	2.105(8)	2.076(8)	2.060(3)
Pd–$S_{(CEES)}$	2.302(4)	2.318(6)	2.300(9)	2.326(17)
$\angle Pl_{(NNNPd)}$–$Pl_{(Ar)}$^{a}	88.3, 89.8	81.0, 83.1	79.8, 85.8	86.7, 86.8

^{a}The angle is defined as the dihedral angle between the side aromatic ring averaged plane and the N(1)N(2)N(3)–Pd pincer averaged plane.

by about 0.02 Å compared to the acetonitrile complexes, an indication of the better trans-directing capabilities of the sulfur donor (see Table S2, Supporting Information). The two proximal phenyl groups are almost orthogonal to the pincer–Pd–S plane for the phenyl pincer,[19] slightly more skewed for the naphthalene complex, and again closer to perpendicular for the anthracene host (dihedral angles about 89°, 82°, and 87°, for the three complexes, respectively). These angles are all much closer to 90° than those found for the three acetonitrile complexes (Table S2, Supporting Information). In all three complexes, the CEES is parallel with the conjugated rings (Figure 4). Although not shown, the bound CEES in each structure exhibited "up-down" disorder, with the chloroethyl and ethyl arms lying in either direction, above or below the pincer plane, so as to resemble an actual bound dichlorodiethyl sulfide, should just the chloroethyl positions be used for the

dx.doi.org/10.1021/ja408770u | J. Am. Chem. Soc. 2013, 135, 17193–17199

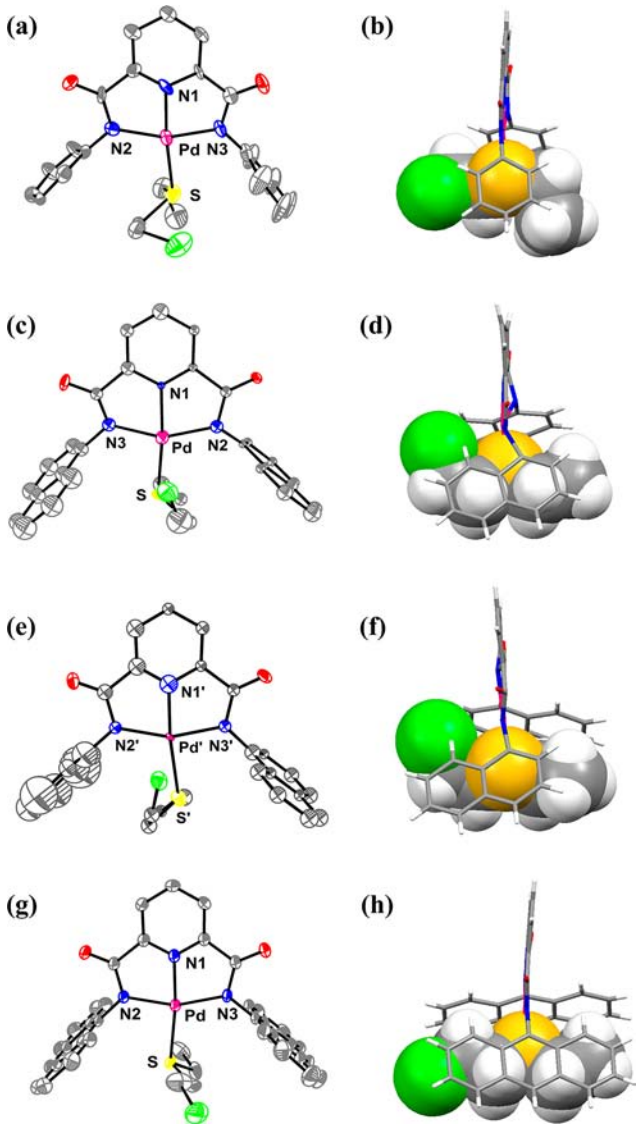

Figure 4. ORTEP drawings at 50% ellipsoid probability and side views showing the bound CEES (space filling) "shielded" by the aromatic walls: Pd($\mathbf{L}^{a}$)(CEES) (a, b); Pd($\mathbf{L}^{e}$)(CEES) (major species **A** (c, d), minor species **C** (e, f)); Pd($\mathbf{L}^{f}$)(CEES) (g, h). Nonessential solvent and water molecules are omitted for clarity.

drawings. However, only the component with a higher occupancy is shown in Figure 4 except for the naphthalene complex (vide infra). What is striking is the increased linear alignment of the mustard surrogate along the aromatic skeleton progressing across the phenyl, naphthalene, anthracene series (Figure 4b,d,f,h).

The structure of Pd($\mathbf{L}^{e}$)(CEES) was complicated because of the cocrystallization of the possible isomers, **A**/**B** and **C** (Scheme 3), which appeared as disordered atomic positions. Upon unraveling the disorder, the two isomers, **A**/**B** and **C**, emerged at about 56% and 44% occupancy, respectively (Figure 4c–f, Table 3, and Supporting Information). Because of the global disorder of the CEES chloroethyl and ethyl positions, the cis isomer could be either **A** or **B**. What is shown in Figure 4c,d is the **A** isomer, because for both the CEES and the pincer portions of the complex, those were the positions with the highest occupancy. Interestingly, the predominant cis form in terms of atom occupancy is opposite to what is identified as the more stable isomer, i.e., trans, in solution over time.

The alignment of the mustard with the naphthalene rings in Pd($\mathbf{L}^{e}$)(CEES) becomes much more apparent compared to the phenyl derivative, Pd($\mathbf{L}^{a}$)(CEES) (Figure 4c–f, and a and b, respectively). However, while the naphthalene falls short of covering the entire surrogate mustard chain, as seen in both Figure 4d,f the chlorine atom wraps up toward the palladium, forming a relatively close contact, 3.10 and 3.16 Å for the **A** and **C** isomers, respectively (Pd···Cl van der Waals contact is about 3.4 Å).[21] This proximity, albeit not an actual bond, constitutes a second interaction of the bound mustard, in addition to the Pd–S bond (or possibly a third interaction if the weak van der Waals attractions with the naphthalene rings are considered). However, it may just be a reflection of the naphthalene orientations, or just happenstance. Nonetheless the Pd···Cl interaction may be in part responsible for the significantly enhanced binding constant compared to the phenyl and phenyl-substituted complexes if it is indeed present in solution.

As anticipated, Pd($\mathbf{L}^{f}$)(CEES) has the same general coordination sphere as the other complexes (Figure 4g and h, Figure 5, and Table 3), although it too suffers from some

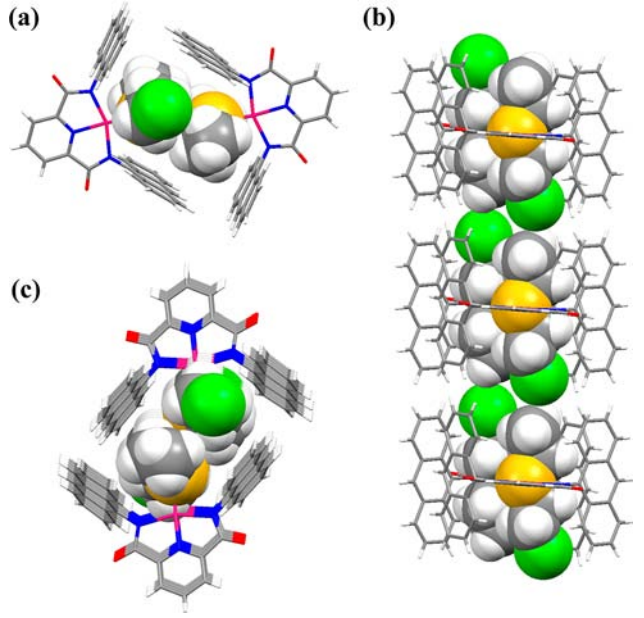

Figure 5. Views of the complex Pd($\mathbf{L}^{f}$)(CEES): (a) four-walled anthracene enclosure of a single dimer pair and (b) overhead and (c) side views of the infinite four-walled channel holding antiparallel head-to-tail CEES chains.

disorder (see Supporting Information). Additionally there is a free CEES of solvation within the crystal lattice that exhibits extreme disorder across the crystallographic inversion center and which resisted all attempts at modeling. Its presence does not, however, detract from the overall validity of the structure of the palladium complex. Clearly, in the anthracene derivative, the extended aromatic rings are beautifully positioned for aligning with the entire length of the mustard carbon chain, with only the chlorine atom poking outside the wall. All the protons on the CEES chain have a short contact with the closest anthracene ring plane (C···π plane distances varying between 3.4 and 3.5 Å), indicating the presence, at the very least, of van der Waals interactions.

dx.doi.org/10.1021/ja408770u | J. Am. Chem. Soc. 2013, 135, 17193–17199

Each Pd($\mathbf{L}^{f}$)(CEES) complex is adjacent to a neighboring complex, forming a dimer pair with the two CEES chains oriented in opposite directions (Figure 5a). The wall-like effects of the anthracene groups then extend throughout the crystal lattice (Figure 5b,c). These findings, that the incorporation of larger aromatic rings results in improved binding affinity as well as the solid-state formation of the extended wall channels, can be potentially expanded to other pseudolinear targets.

CONCLUSIONS

The goal of this project was to examine the influence of peripheral groups attached to NNN pincer complexes of Pd(II) on the binding of the pseudolinear sulfur mustard surrogate CEES. The ligands are readily synthesized by an efficient, high-yield two-step reaction, followed by complexation with palladium(II). The acetonitrile complexes were found to bind CEES, rapidly forming an equilibrium between free and complexed guest. The high affinity of the palladium complexes for CEES was anticipated due to the soft nature of both the palladium and sulfur atoms, in keeping with hard−soft−acid−base concepts. Unanticipated, however, was the extent of the other potential interactions of the CEES with the pincer framework that led to a surprising range of values for the equilibrium constants. While simple substituents on the side phenyl rings resulted only in slight enhancements of binding, the incorporation of more extended aromatic rings, e.g., naphthalene and anthracene, provided more rigid structural "walls" to enclose the pseudolinear guest and significantly enhanced binding.

Furthermore, with the help of NMR spectroscopy, an interesting interplay of cis and trans isomers was identified in the naphthalene CEES derivative. Findings indicated not only that isomerization may be occurring in solution but also that the mechanism might proceed via a preferred CEES addition to the cis rather than trans precursor complex. These results are currently being explored further.

This study has thus shed light on detailed structural and mechanistic aspects of the binding of pseudolinear molecules with square planar pincer complexes. While structural complementarity in terms of host−guest interactions has long been known, the clearly identified wall effect observed with the mustard surrogate may lead to new applications of wall-building in sensing, separations, and transport of other target molecules and ions.

ASSOCIATED CONTENT

Supporting Information

Crystallographic data in CIF format. Synthetic procedures and spectral characterization of compounds, NMR studies, and crystallographic information. This material is available free of charge via the Internet at http://pubs.acs.org.

AUTHOR INFORMATION

Corresponding Author

kbjames@ku.edu

Notes

The authors declare no competing financial interest.

ACKNOWLEDGMENTS

This project received support from the Defense Threat Reduction Agency-Joint Science and Technology Office for Chemical and Biological Defense (B104283I). The authors also thank the National Science Foundation, CHE-0923449 for purchase of the X-ray diffractometer. We also thank Dr. J. T. Douglas for NMR technical assistance and helpful discussion.

REFERENCES

(1) Marshall, E. K., Jr. *J. Am. Med. Assoc.* **1919**, *73*, 684−686.
(2) (a) Jackson, K. E. *Chem. Rev.* **1934**, *15*, 425−462. (b) Sartori, M. F. *Chem. Rev.* **1951**, *48*, 225−257.
(3) (a) Gilman, A.; Philips, F. S. *Science* **1946**, *103*, 409−436. (b) Goodman, L. S.; Wintrobe, M. M.; Dameshek, W.; Goodman, M. J.; Gilman, M. A.; Mclennan, M. T. *J. Am. Med. Assoc.* **1946**, *132*, 126−132.
(4) (a) Goodman, L. S.; Wintrobe, M. M.; Dameshek, W.; Goodman, M. J.; Gilman, M. A.; McLennan, M. T. *J. Am. Med. Assoc.* **1984**, *251*, 2255−2261. (b) Frunzi, J. *The Hospitalist*; Society of Hospital Medicine: Philadelphia, February 2007.
(5) Wang, Q.-Q.; Begum, R. A.; Day, V. W.; Bowman-James, K. *Org. Biomol. Chem.* **2012**, *10*, 8786−8793.
(6) (a) Somani, S. M; Babu, S. R. *Int. J. Clin. Pharmacol. Ther. Toxicol.* **1989**, *27*, 419−435. (b) Malhotra, R. C.; Ganesan, K.; Sugendran, K.; Swamy, R. V. *Def. Sci. J.* **1999**, *49*, 97−116.
(7) (a) Yang, Y.-C.; Baker, J. A.; Ward, J. R. *Chem. Rev.* **1992**, *92*, 1729−1743. (b) Munro, N. B.; Talmage, S. S.; Griffin, G. D.; Waters, L. C.; Watson, A. P.; King, J. F.; Hauschild, V. *Environ. Health Perspect.* **1999**, *107*, 933−974. (c) Smith, B. M. *Chem. Soc. Rev.* **2008**, *37*, 470−478.
(8) (a) Ware, D. C.; Palmer, B. D.; Wilson, W. R.; Denny, W. A. *J. Med. Chem.* **1993**, *36*, 1839−1846. (b) Craig, P. R.; Brothers, P. J.; Clark, G. R.; Wilson, W. R.; Denny, W. A.; Ware, D. C. *Dalton Trans.* **2004**, 611−618. (c) Blower, P. J.; Dilworth, J. R.; Maurer, R. I.; Mullen, G. D.; Reynolds, C. A.; Zheng, Y. *J. Inorg. Biochem.* **2001**, *85*, 15−22. (d) Parker, L. L.; Lacy, S. M.; Farrugia, L. J.; Evans, C.; Robins, D. J.; O'Hare, C. C.; Hartley, J. A.; Jaffar, M.; Stratford, I. J. *J. Med. Chem.* **2004**, *47*, 5683−5689. (e) Wu, J.; Huang, R.; Wang, T.; Zhao, X.; Zhang, W.; Weng, X.; Tian, T.; Zhou, X. *Org. Biomol. Chem.* **2013**, *11*, 2365−2369.
(9) (a) Burnworth, M.; Rowan, S. J.; Weder, C. *Chem.—Eur. J.* **2007**, *13*, 7828−7836. (b) Royo, S.; Martínez-Máñez, R.; Sancenón, F.; Costero, A. M.; Parra, M.; Gil, S. *Chem. Commun.* **2007**, 4839−4847. (c) Kim, K.; Tsay, O. G.; Atwood, D. A.; Churchill, D. G. *Chem. Rev.* **2011**, *111*, 5345−5403.
(10) (a) Montoro, C.; Linares, F.; Procopio, E. Q.; Senkovska, I.; Kaskel, S.; Galli, S.; Masciocchi, N.; Barea, E.; Navarro, J. A. R. *J. Am. Chem. Soc.* **2011**, *133*, 11888−11891. (b) Sambrook, M. R.; Hiscock, J. R.; Cook, A.; Green, A. C.; Holden, I.; Vincent, J. C.; Gale, P. A. *Chem. Commun.* **2012**, *48*, 5605−5607.
(11) Kumar, V.; Anslyn, E. V. *J. Am. Chem. Soc.* **2013**, *135*, 6338−6344.
(12) (a) Albrecht, M.; van Koten, G. *Angew. Chem., Int. Ed.* **2001**, *40*, 3750−3781. (b) van der Boom, M. E.; Milstein, D. *Chem. Rev.* **2003**, *103*, 1759−1792. (c) Singleton, J. T. *Tetrahedron* **2003**, *59*, 1837−1857. (d) *The Chemistry of Pincer Compounds*; Morales-Morales, D., Jensen, C. M., Eds; Elsevier: Amsterdam, 2007. (e) Leis, W.; Mayer, H. A.; Kaska, W. C. *Coord. Chem. Rev.* **2008**, *252*, 1787−1797.
(13) (a) Serrano-Becerra, J. M.; Morales-Morales, D. *Curr. Org. Synth.* **2009**, *6*, 169−192. (b) Choi, J.; MacArthur, A. H. R.; Brookhart, M.; Goldman, A. S. *Chem. Rev.* **2011**, *111*, 1761−1779. (c) Selander, N.; Szabó, K. J. *Chem. Rev.* **2011**, *111*, 2048−2076. (d) Pincers and Other Hemilabile Ligands, Themed Issue: *Dalton Trans.* **2011**, *40* (35).
(14) (a) Hossain, M. A.; Lucarini, S.; Powell, D.; Bowman-James, K. *Inorg. Chem.* **2004**, *43*, 7275−7277. (b) Begum, R. A.; Powell, D.; Bowman-James, K. *Inorg. Chem.* **2006**, *45*, 964−966.
(15) (a) Moriuchi, T.; Bandoh, S.; Miyaji, Y.; Hirao, T. *J. Organomet. Chem.* **2000**, *599*, 135−142. (b) Moriuchi, T.; Bandoh, S.; Miyaishi, M.; Hirao, T. *Eur. J. Inorg. Chem.* **2001**, 651−657. (c) Moriuchi, T.; Kamikawa, M.; Bandoh, S.; Hirao, T. *Chem. Commun.* **2002**, 1476−1477.

(16) Dell'Amico, D. B.; Calderazzo, F.; Colo, F. D.; Guglielmetti, G.; Labella, L.; Marchetti, F. *Inorg. Chim. Acta* **2006**, *359*, 127−135.
(17) Reed, J. E.; White, A. J. P.; Neidle, S.; Vilar, R. *Dalton Trans.* **2009**, 2558−2568.
(18) Pérez, Y.; Johnson, A. L.; Raithby, P. R. *Polyhedron* **2011**, *30*, 284−292.
(19) Wang, Q.-Q.; Begum, R. A.; Day, V. W.; Bowman-James, K. *Inorg. Chem.* **2012**, *51*, 760−762.
(20) Wang, Q.-Q.; Day, V. W.; Bowman-James, K. *Chem. Commun.* **2013**, *49*, 8042−8044.
(21) Bondi, A. *J. Phys. Chem.* **1964**, *68*, 441−451.